

Melamine holding PbI_2 with three “arms”: an effective chelation strategy to control the lead iodide to perovskite conversion for inverted perovskite solar cells

*Shizi Luo,^{ab} Shuguang Cao,^{ab} Tongjun Zheng,^{ab} Zhuoneng Bi,^b Yupeng Zheng,^b Yiqun Li,^{ab} Biniyam Zemene Taye,^{abf} Victoria V. Ozerova,^c Lyubov A. Frolova,^c Nikita A. Emelianov,^c Eugeny D. Tarasov,^c Zheng Liang,^{*b} Lavrenty G. Gutsev,^{*ce} Sergey M. Aldoshin,^c Bala R. Ramachandran,^e Pavel A. Troshin,^{*dc} Xueqing Xu^{*ab}*

^a *School of Energy Science and Engineering, University of Science and Technology of China, Hefei, 230026, P.R. China*

^b *Key Laboratory of Renewable Energy, Guangdong Provincial Key Laboratory of New and Renewable Energy Research and Development, Guangzhou Institute of Energy Conversion, Chinese Academy of Sciences, Guangzhou 510640, P.R. China*

^c *Federal Research Center for Problems of Chemical Physics and Medicinal Chemistry, Russian Academy of Sciences (FRC PCP MC RAS), Academician Semenov av. 1, Chernogolovka, Moscow region 142432, Russia*

^d *Zhengzhou Research Institute of HIT, 26 Longyuan East 7th, Jinshui District, Zhengzhou, Henan Province, 450000, China*

^e *Institute for Micromanufacturing, Louisiana Tech University, Ruston, LA 71272, United States*

^f *Faculty of Electrical and Computer Engineering, Bahir Dar Institute of Technology, Bahir Dar University, Bahir Dar, P.O. Box 26 Ethiopia*

* Corresponding authors.

E-mail addresses:

xuxq@ms.giec.ac.cn (X. Xu);

Keywords: Melamine, Tridentate chelation PbI_2 , Synergistic effect, Sequential deposition method, Inverted perovskite solar cells

1. Materials

Dimethylformamide (DMF, >99%), dimethyl sulfoxide (DMSO, >99.5%), chlorobenzene (CB, anhydrous, 99.8%) were purchased from Sigma-Aldrich. Isopropyl alcohol (IPA, anhydrous, 99.8%) was purchased from Acros. The NiO_x powder, lead iodide (PbI₂, 99.99%) and lead bromide (PbBr₂) were purchased from Advanced Election Technology Co., Ltd. CsI, [6,6]-Phenyl-C₆₁-butyric acid methyl ester (PCBM), 2,9-Dimethyl-4,7-diphenyl-1,10-phenanthroline (BCP), methylammonium chloride (MACl), formamidinium iodide (FAI) and methylammonium bromide (MABr) were purchased from Xi'an Yuri Solar Co., Ltd. [4-(3,6-Dimethyl-9H-carbazol-9-yl)butyl]phosphonic Acid (Me-4PACz) was purchased from Acros (TCI). Melamine (MEA) was purchased from Aladdin.

2. Fabrication of Rigid Small-Area PSCs

The ITO-coated glass substrates (purchased from Wuhan Lattice Solar Energy Technology Co. LTD.) were ultrasonically cleaned with soap solution, deionized water, ethanol and isopropyl alcohol each for 20 min, respectively, and then dried under a stream of nitrogen. The pre-cleaned ITO/glass substrates were treated with UV-Ozone (UVO) for 15 min to remove the organic residue. The NiO_x nanoparticle solution (10 mg/mL) was spin-coated onto the ITO/glass substrates at 2000 rpm for 30 s and annealed for 10 min at 150°C, then quickly transferred to a glove box. Me-4PACz (0.3 mg/mL in ethanol) was spin-coated on NiO_x at 4000 rpm for 30 s, annealed for 10 min at 100°C and cooled for 5 min.

PbI₂ powder (1.5 M) in mixed solvent (DMF and DMSO with volume ratio of 9:1) was dropped onto the HTL and spin-coated at 2500 rpm for 30 s, then annealed for 1 min at 70°C. The perovskite films modified with CsI, MEA or CsI&MEA were prepared by adding 75 mM CsI, 2.5 mg/ml MEA or both in PbI₂ precursor, respectively.

Notably, the solution of PbI_2 precursor with MEA was required to be continuously heated at 70°C to preserve its transparency and suppressing the formation of precipitates. Organic salts solution (FAI/MAI/MACl (90:6.4:10 mg) in 1 mL IPA was dynamically dropped onto the PbI_2 film after 5 s of the process starting at 3500 rpm for 35 s, and then annealed for 50 min at 100°C . For post-treatment, 1 mg/mL PEAI in mixed solvent (IPA: DMSO=150: 1) was dynamically spin-coated onto the perovskite surface with 4000 rpm for 30 s, and then annealed for 5 min at 100°C . Next, 20 mg/mL PCBM in CB and 0.5 mg/mL BCP in IPA was spin coated at 4000 rpm for 30 s, respectively. Finally, the Ag top electrode (100 nm) was deposited by thermal evaporation in vacuum through a shadow mask defining the device active area as 0.048 cm^2 .

3. Fabrication of flexible perovskite solar cells

The PEN/ITO substrates were sequentially cleaned with soap solution, deionized water, ethanol and isopropyl alcohol each for 20 min, respectively, by using an ultrasonic water bath and dried in a nitrogen flow. Maintaining the flatness of the flexible substrate during device manufacturing is the key to achieve highly efficient flexible PSCs. Attaching the flexible substrates to the glass substrate and using PDMS for mechanical support. The cleaned PEN/ITO substrate was treated with O_2 PLASMA for 15 min. The latter processing is the same as for the preparation of the perovskite solar cells with rigid substrates.

4. Characterizations

The perovskite films were characterized by X-ray photoelectron spectroscopy (XPS, ESCALAB 250Xi, Thermo Scientific K-Alpha). Ultraviolet photoelectron spectra (UPS) were also measured by Thermo Scientific ESCALAB 250Xi, with the HeI (21.22 eV) emission line employed for excitation. The surface microstructure of perovskite films and the cross-sectional images of PSCs were obtained using SU-70 high-resolution analytical SEM (Hitachi, Japan). PL and TRPL spectra of perovskite films

were obtained using Edinburgh fluorescence spectrometer (FLS980). The X-ray diffraction (XRD) patterns of perovskite films were obtained using X'Pert PRO MPD X-Ray diffractometer with Cu K α irradiation at a scan rate (2θ) of 0.0167 $^{\circ}$ S $^{-1}$. For J - V measurements, the intensity of the light was 100 mW cm $^{-2}$ (simulated AM 1.5 G) provided by ABET Sun 3000 solar simulator and calibrated by a standard silicon reference cell. Grazing incidence X-ray diffraction (GIXRD) was performed using Rigaku SmartLab. Atomic force microscopy (AFM) measurements were performed by Bruker Multimode. The IR s-SNOM measurements were carried out using a neaSNOM microscope (Neaspec, Haar, Germany) in PsHet mode with a Mid-IR laser MIRcat-2400 (Daylight Solutions, USA) installed inside the MBraun glove box (O_2 , H_2O < 0.1 ppm). The J - V curves, space charge-limited current (SCLC) and electrochemical impedance spectroscopy (EIS) measurements for the solar cells were performed using Autolab TYPE II electrochemical work station. The external quantum efficiency (EQE) spectra of the solar cells were obtained using QTest Hifinity 5 (Crowntech, USA). The operational stability of the FPSCs was studied at maximum power point tracking (MPPT) using a 100 mW cm $^{-2}$ white LED lamp (Suzhou D&R Instrument Co., Ltd.) in an N $_2$ -filled glove box.

5. Density Functional Theory Calculations

For molecular docking calculations we used the GAUSSIAN 09 suite of programs with the hybrid B3LYP functional and the 6-311G* basis set for organic atoms as well as Lanl2Dz basis set for Pb and I. The D3 dispersion correction was also included.¹ To perform the docking calculation we took a monolayer PbI $_2$ (ML-PbI $_2$) and cut a 5x5x1 cluster (Pb $_{25}$ I $_{50}$). Either a single melamine (MEA) or two MEA were docked onto the various possible sites (I-rich, Pb-moderate, Pb-rich) of the ML-PbI $_2$ cluster. Only the melamines were allowed to geometrically relax while the PbI $_2$ was kept frozen, this is related to the fact that the terminations of such a small ML-PbI $_2$ cluster will make the cluster lose integrity by forming I $_3$ chains and Pb(0) at the terminations. The adsorption energy of the MEA on the PbI $_2$ cluster was calculated as:

$$E_{ads}(D^q) = E_{PbI_2/pass}(D^q) - E_{PbI_2}(D^q) - E_{pass} \quad (7)$$

where D^q either indicates whether the species is pristine or defective. $E_{PbI_2/pass}$ is the energy of the PbI_2 cluster with passivant added, E_{PbI_2} is the passivant-free PbI_2 cluster and E_{pass} is the energy of the passivant (MEA).

To perform MEA adsorption calculations on the surface of perovskites we used the Vienna Ab initio Simulation Package (VASP) of programs.² The α -FAPbI₃ (100) surface was used as our base to build supercells. For convenience, we further consider the (100) direction as the “z-axis”. By this convention we built supercells with a dimension of 3×3×5 which we previously found to be a decent compromise in quality and computational speed. A vacuum of 20 Å was added above the surface of FAPI to minimize interactions between periodic images. The calculation was done with a full relaxation of atomic and lattice constants with only the restriction that the cell volume remains constant.

The calculations were performed with Gamma-point sampling of the momentum space and then improved to 2 x 2 x 1 . The PBE functional was used and, just as in the case of the molecular calculations, combined with D3 dispersion correction.^{3, 4} The projector augmented-wave (PAW) pseudopotentials were used and we chose an energy cut-off of the plane-wave component of 520 eV,^{5, 6} an increase to 650 eV did not produce a noticeable change in energies indicating that our chosen value is sufficient. Also, we included the so-called non-spherical contributions to the gradient inside the PAW spheres. These corrections have shown improvement when simulating the observables of perovskite oxides.⁷ For adsorption calculations we used equation (1) except the PbI_2 is to be replaced with FAPbI₃.

6. Figures and tables

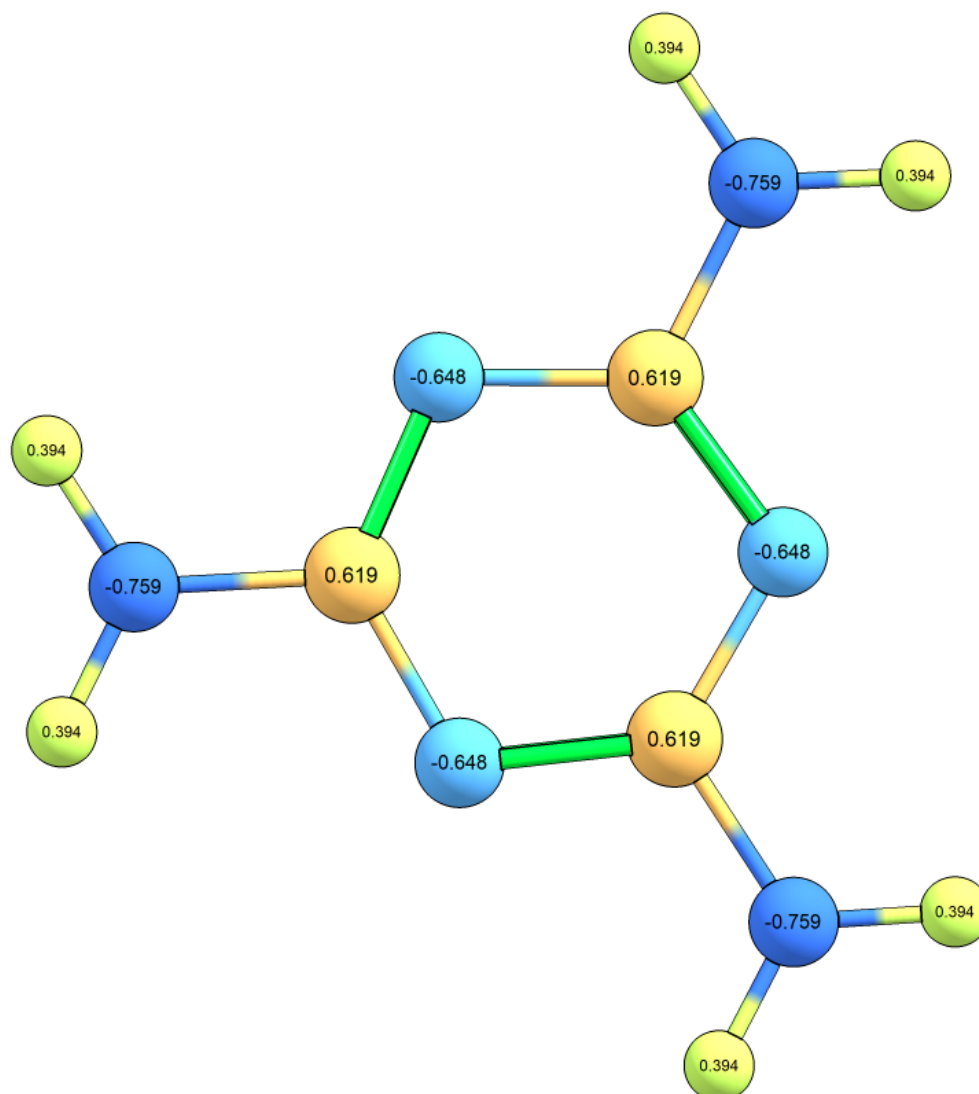


Fig. S1 NBO charges of Melamine molecule localized to atoms where red is negative, blue is positive and green is neutral with a charge color range of -0.5 to 0.5.

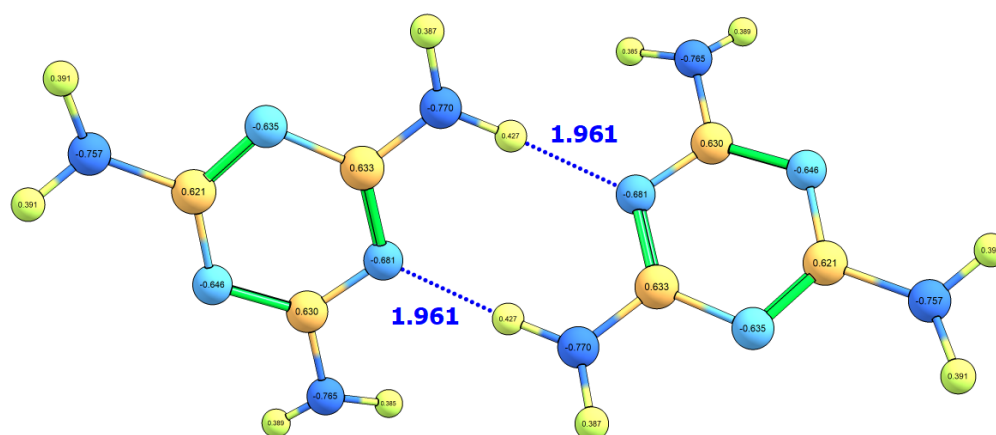


Fig. S2 Dimerization of a melamine salt pair with itself via a double NH₂-N(azine) hydrogen bond and the corresponding NBO charges localized to atoms where red is negative, blue is positive and green is neutral with a charge color range of -0.5 to 0.5.. The dimerization energy is predicted to be -0.59 eV at the B3LYP/6-311+G* level. When compared to Fig. S1 we note the notable charge transfer between NH₂-N(azine).

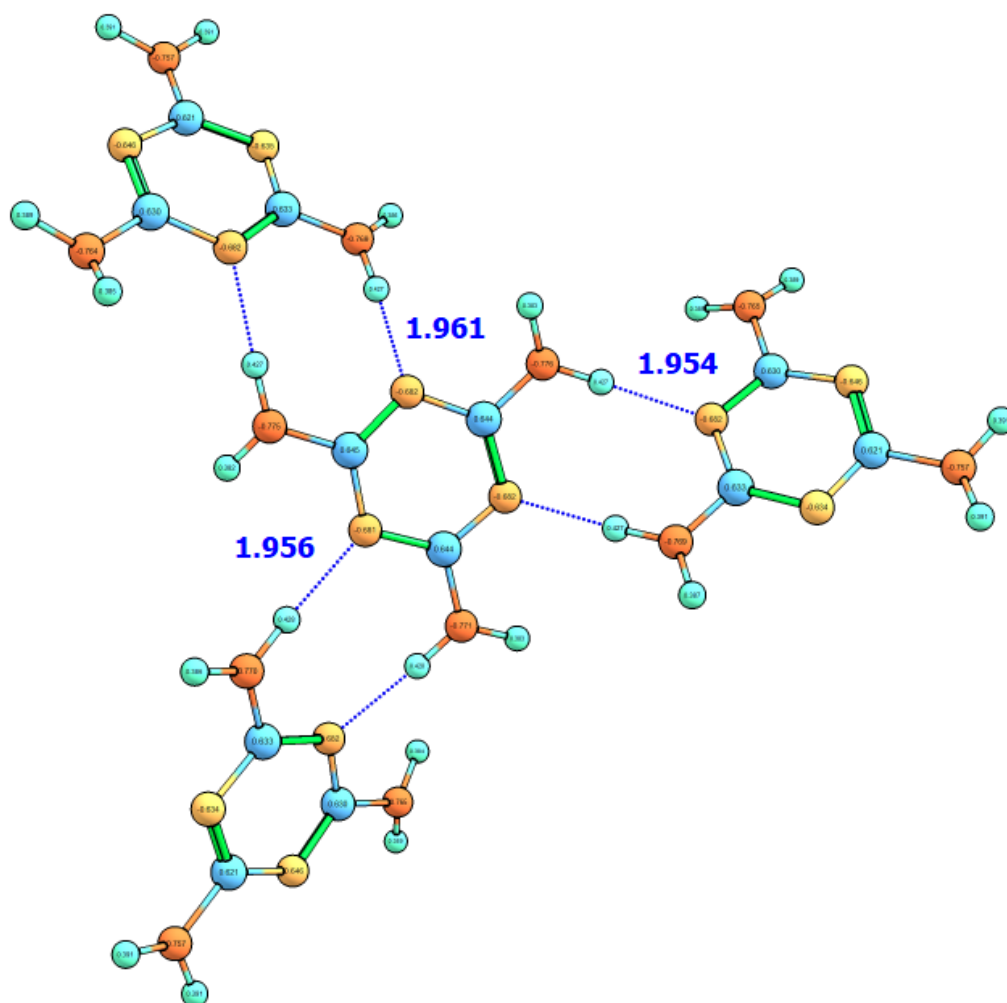


Fig. S3 Tetramerization of two melamine salt dimers via double NH₂-N(azine) hydrogen bond and the corresponding NBO charges localized to atoms where red is negative, blue is positive and green is neutral. The dimerization energy is predicted to be -0.88 eV per dimer at the B3LYP/6-311+G* level. When compared to Fig. S1 we note the significant charge transfer between NH₂-N(azine).

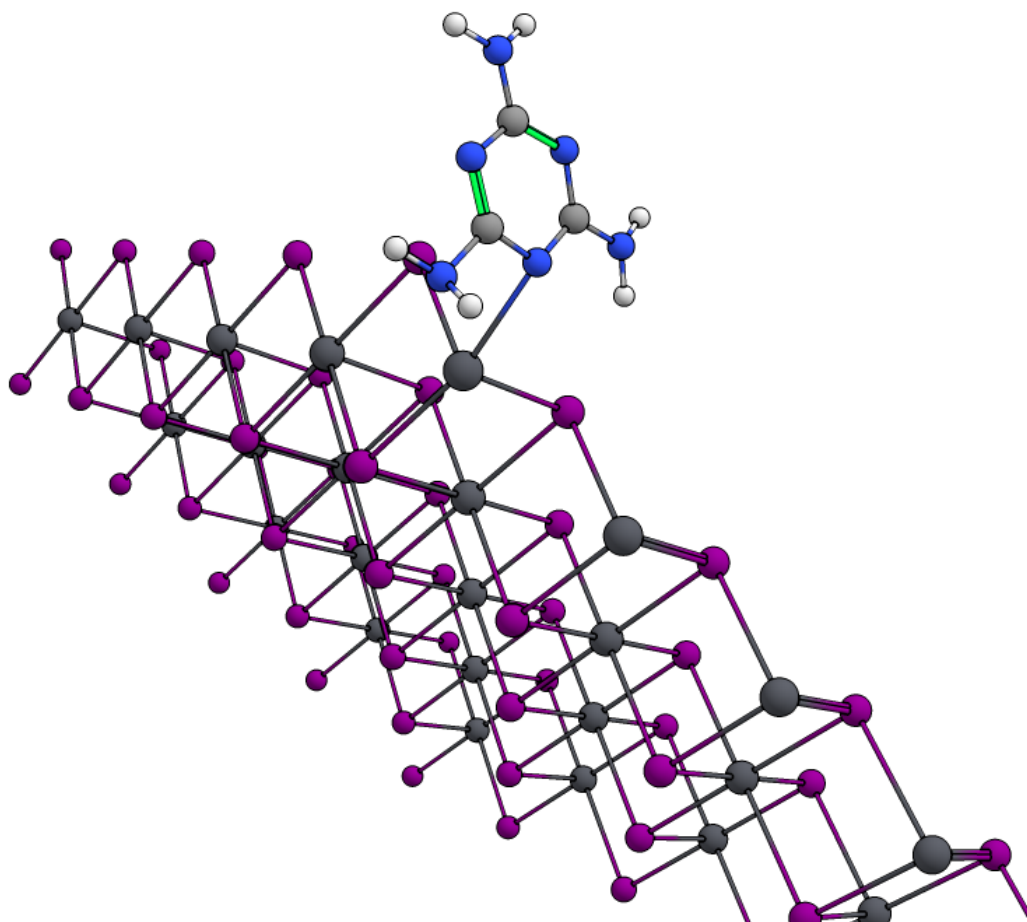
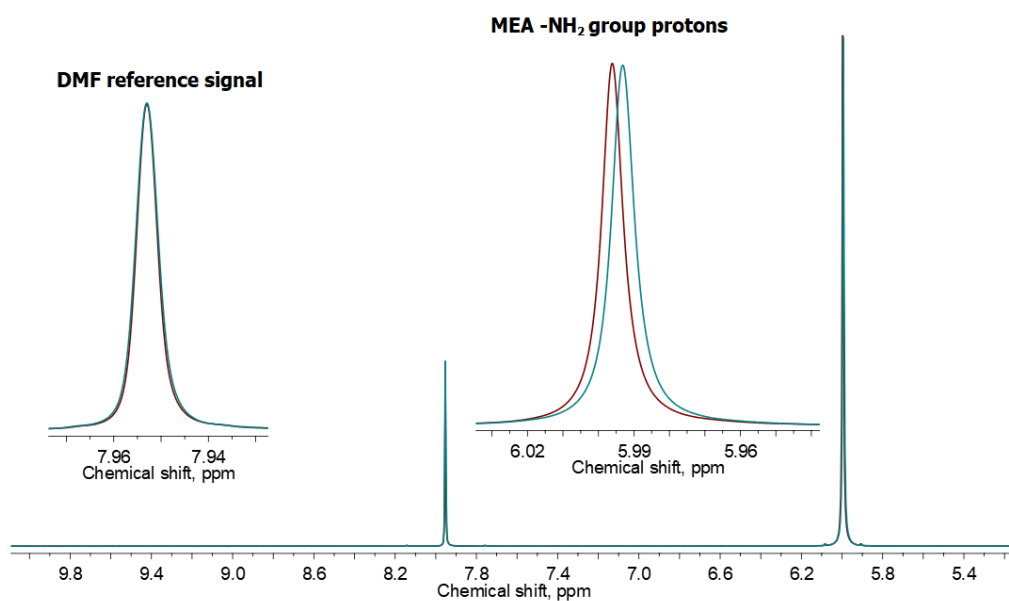


Fig. S4 Passivation of a 5 x 5 x 1 ML-PbI₂ supercell by 1 MEA (Pb-rich termination). This was the most energetically-favorable docking of a single MEA molecule among many others tested.

a



b

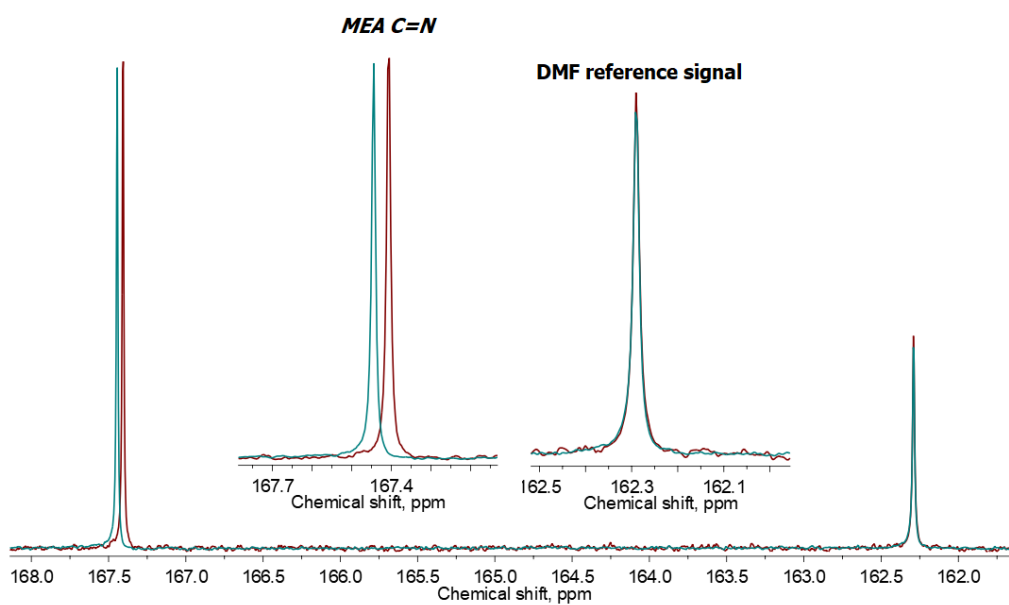


Fig. S5 Comparison of the ¹H (a) and ¹³C (b) NMR spectra of individual MEA solution (cyan) and MEA+PbI₂ equimolar mixture solution (red) in DMSO-d₆ with the addition of DMF as internal standard.

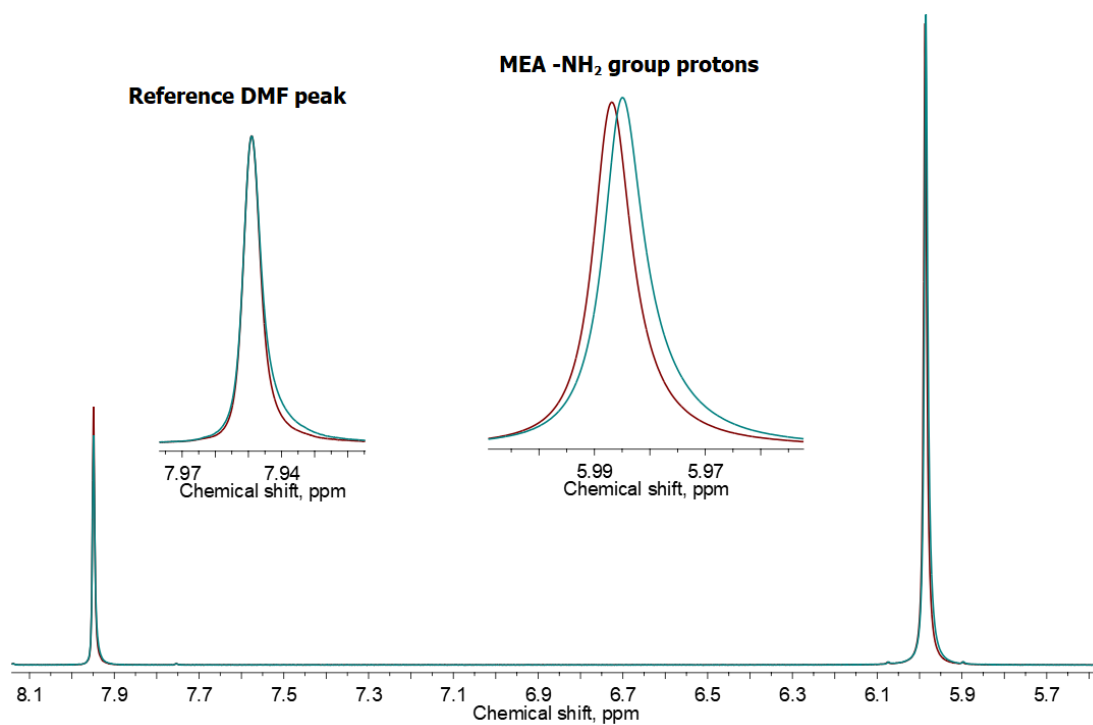


Fig. S6 Comparison of the ¹H NMR spectra of individual MEA solution (cyan) and MEA+CsI equimolar mixture solution (red) in DMSO-d₆ with the addition of DMF as internal standard.

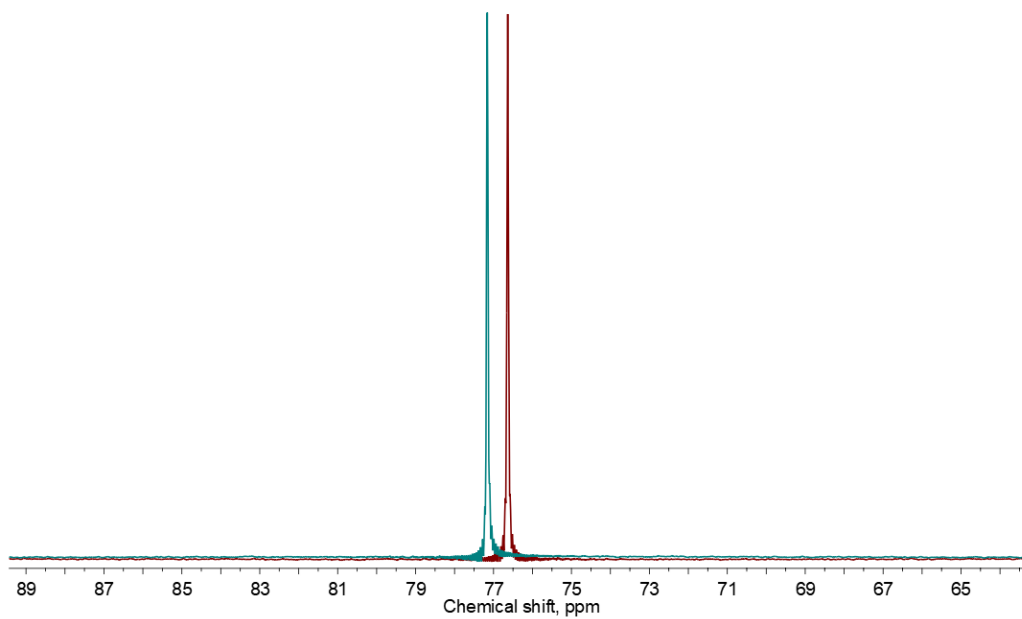


Fig. S7 Comparison of the ^{133}Cs NMR spectra of individual CsI solution (cyan) and MEA+CsI equimolar mixture solution (red) in DMSO- d_6 with the addition of DMF as internal standard.

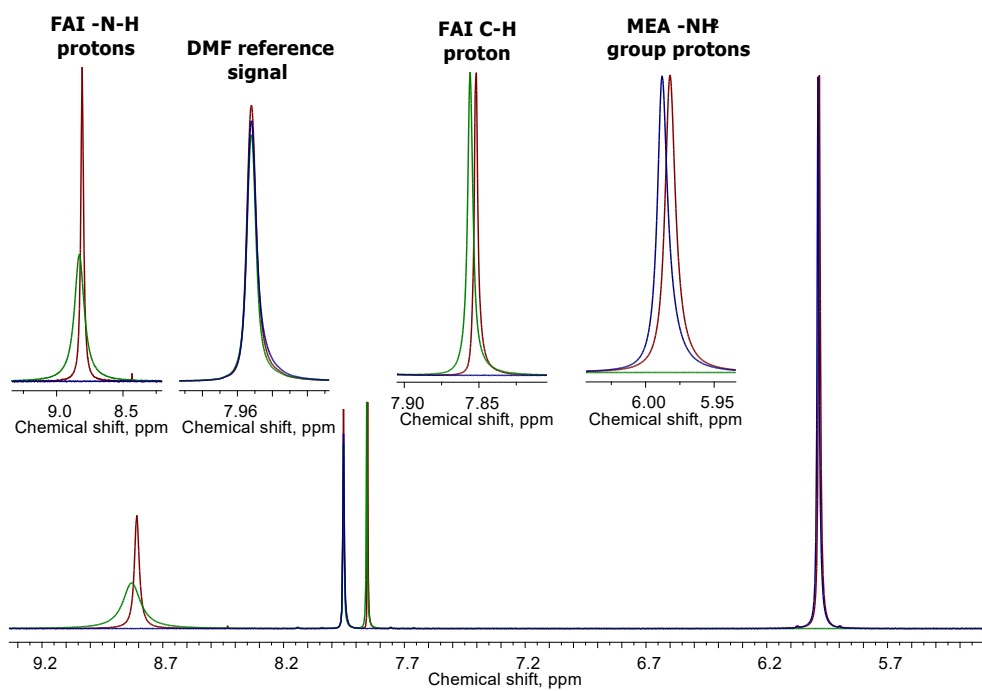


Fig. S8 Comparison of the ¹H NMR spectra of individual solutions of FAI (green), MEA (blue) and MEA+FAI equimolar mixture solution (red) in DMSO-d₆ with the addition of DMF as internal standard.

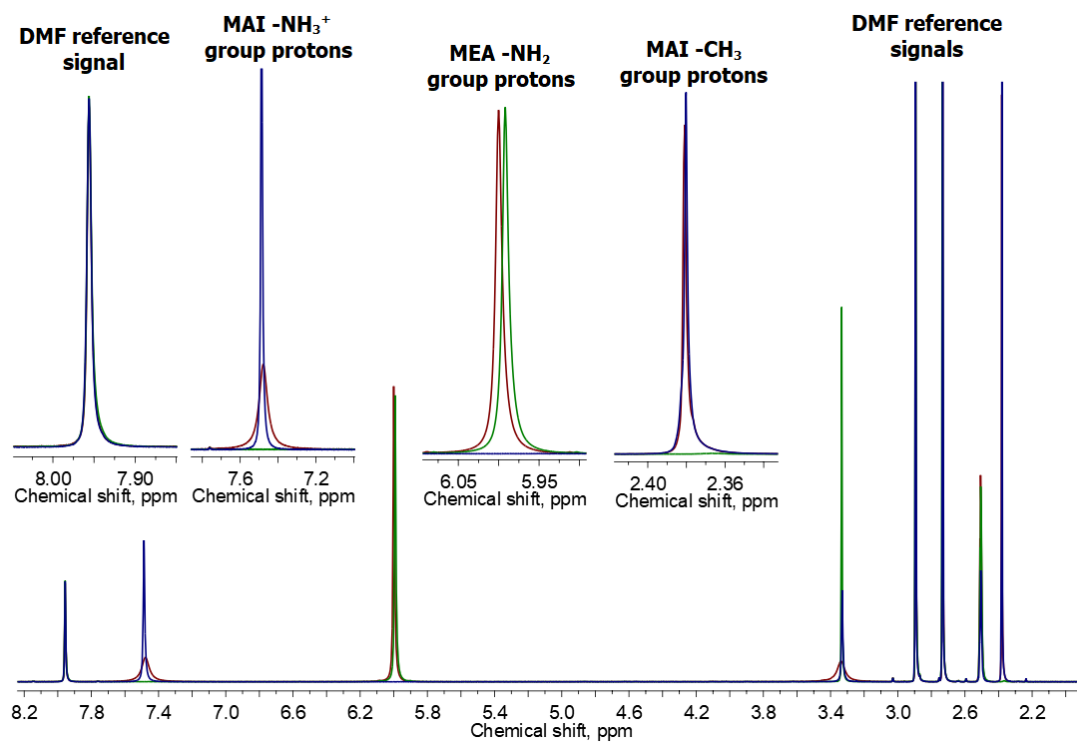


Fig. S9 Comparison of the ¹H NMR spectra of individual solutions of MAI (blue), MEA (green) and MEA+MAI equimolar mixture solution (red) in DMSO-d₆ with the addition of DMF as internal standard.

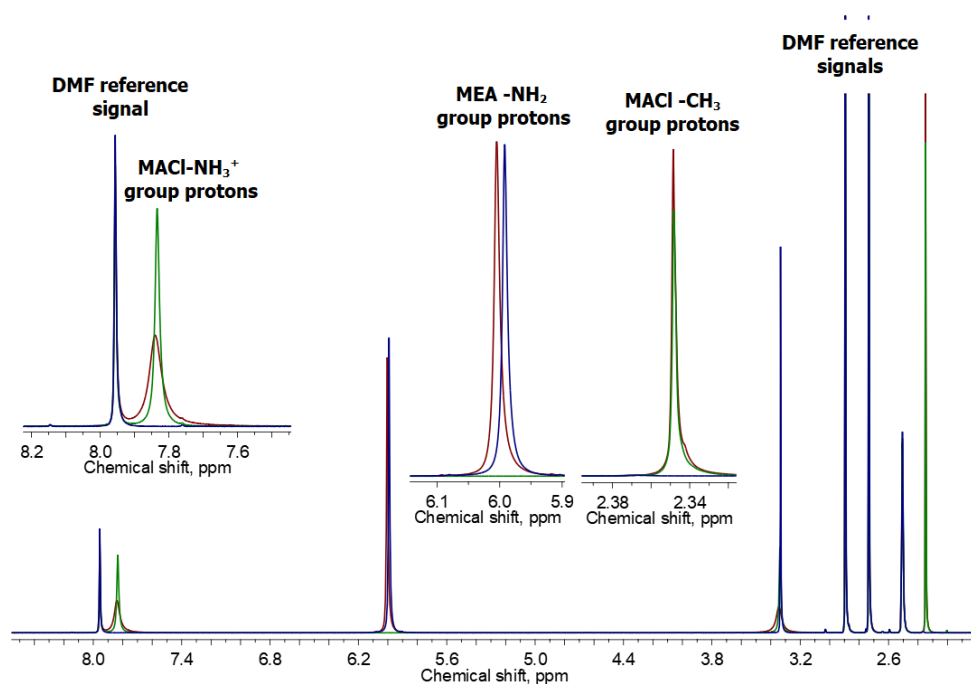


Fig. S10 Comparison of the ^1H NMR spectra of individual solutions of MACI (green), MEA (blue) and MEA+MAI equimolar mixture solution (red) in DMSO- d_6 with the addition of DMF as internal standard.

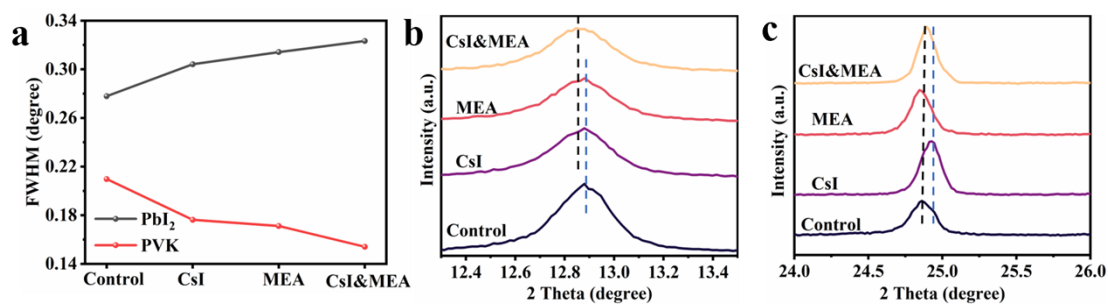


Fig. S11 (a) FWHMs of the first XRD peak for the differently processed PbI_2 films and the (111) diffraction peak in the differently processed perovskite films. (b) Zoom of the first PbI_2 diffraction peak of the differently processed PbI_2 films. (c) Zoom of the (111) diffraction peak of the differently processed perovskite films.

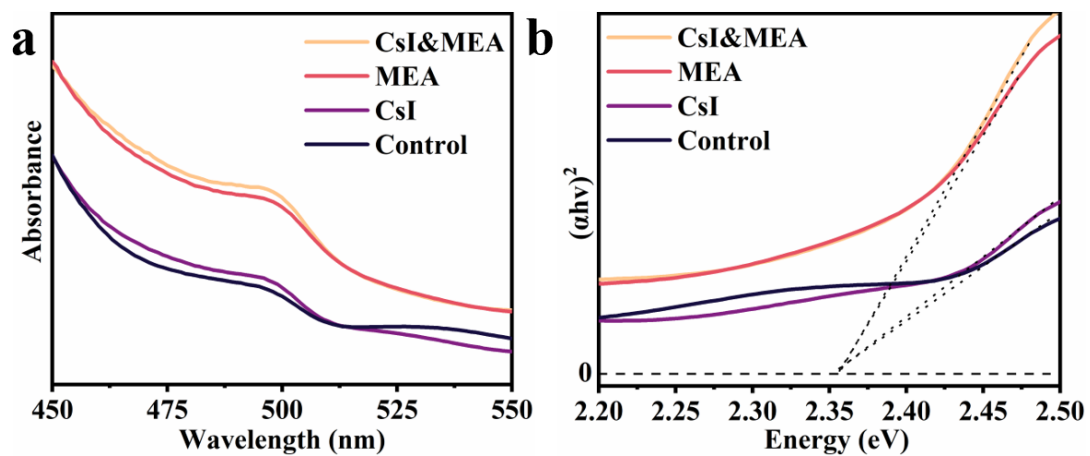


Fig. S12 (a) UV-vis absorption spectroscopy and (b) the optical bandgaps of differently processed PbI₂ films.

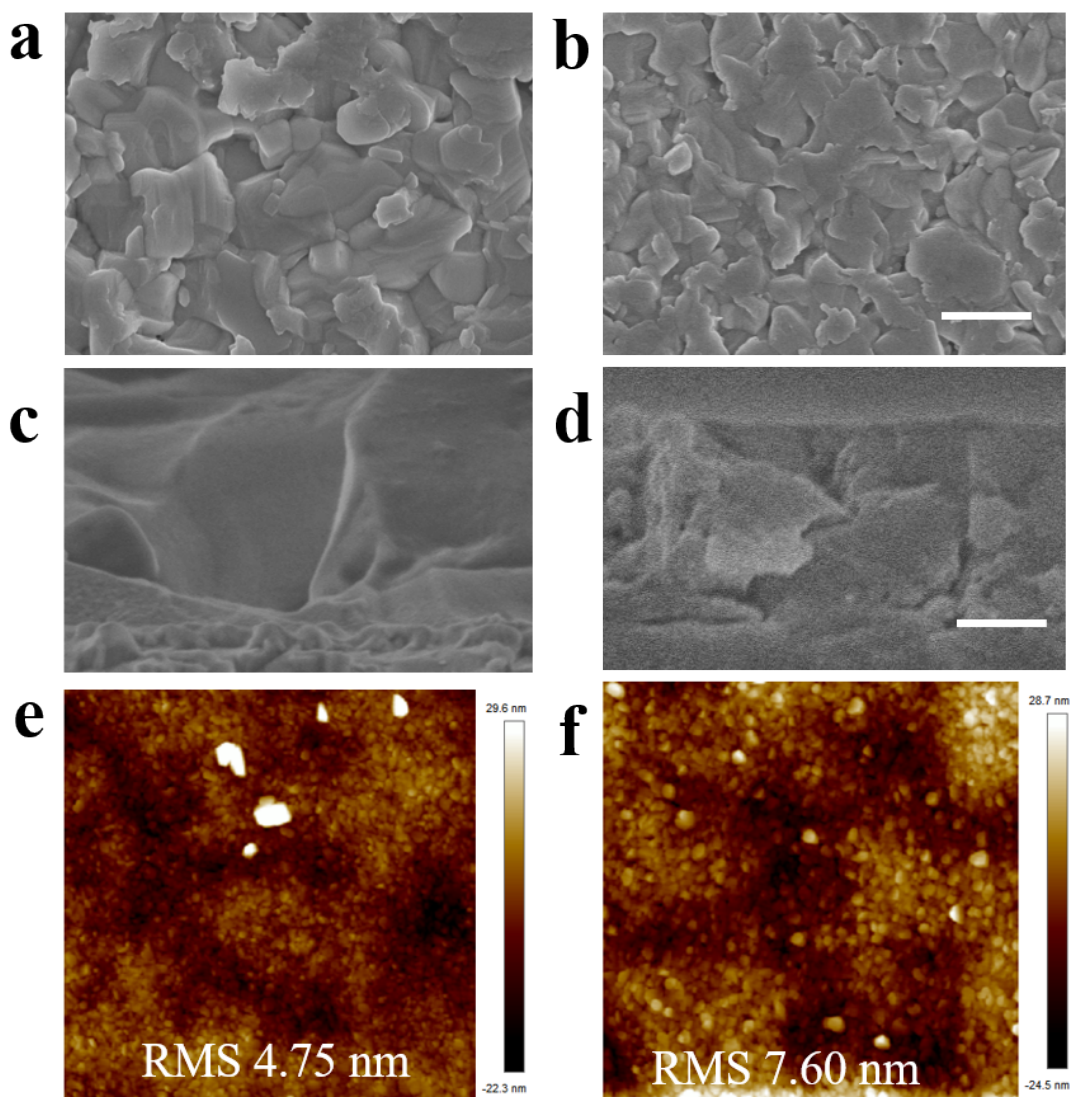


Fig. S13 (a-b) Top view (the scale bar is 200 nm) and (c-d) cross-sectional SEM images (the scale bar is 200 nm) and (e, f) AFM topography images of PbI_2 (left) and PbI_2+MEA (right) films ($5\ \mu\text{m} \times 5\ \mu\text{m}$).

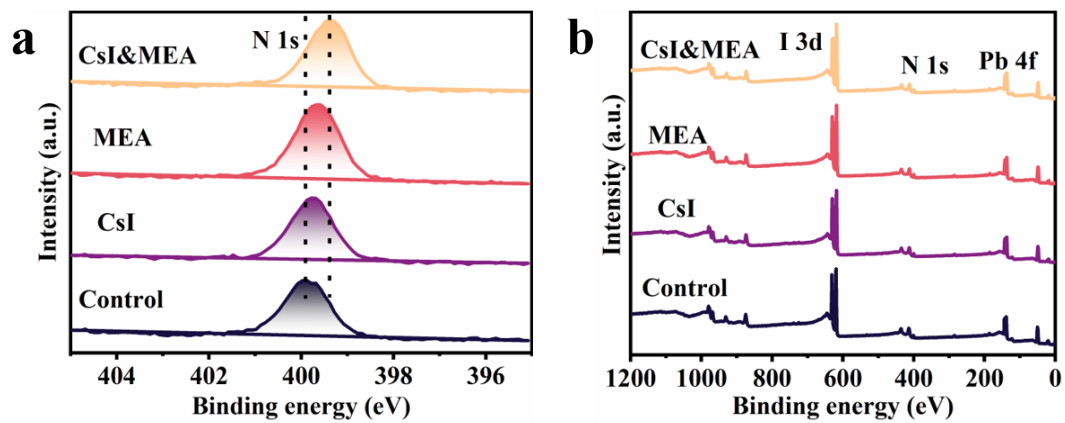


Fig. S14 (a) N 1s XPS core level and (b) survey XPS spectra of differently prepared perovskite films.

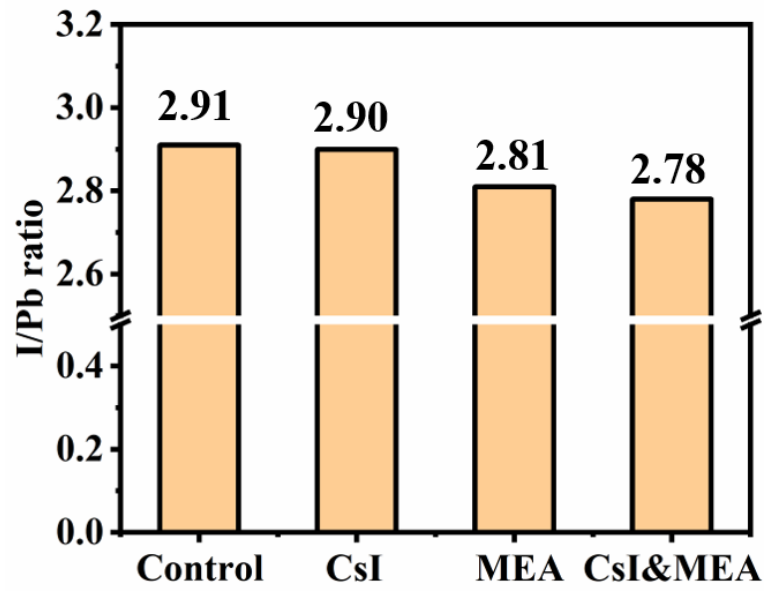


Fig. S15 The I/Pb atomic ratio on the surface of differently processed perovskite films.

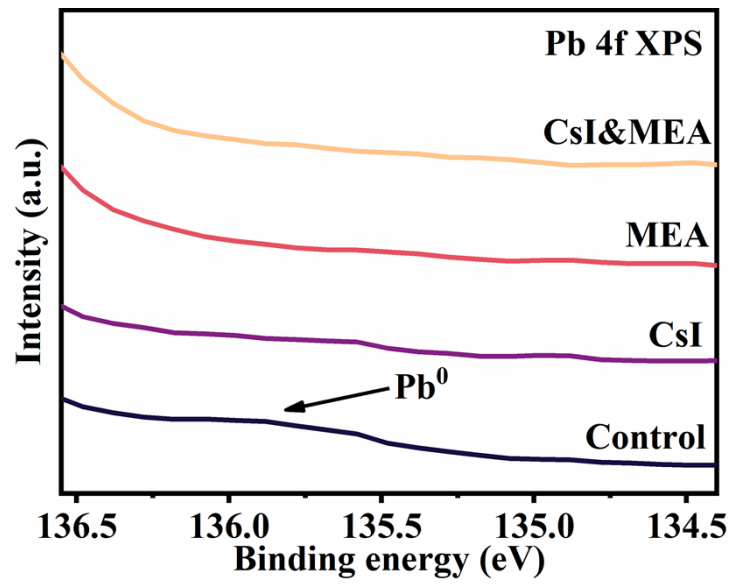


Fig. S16 Pb 4f XPS core level spectra at the binding energy of around 136 eV for differently processed perovskite films.

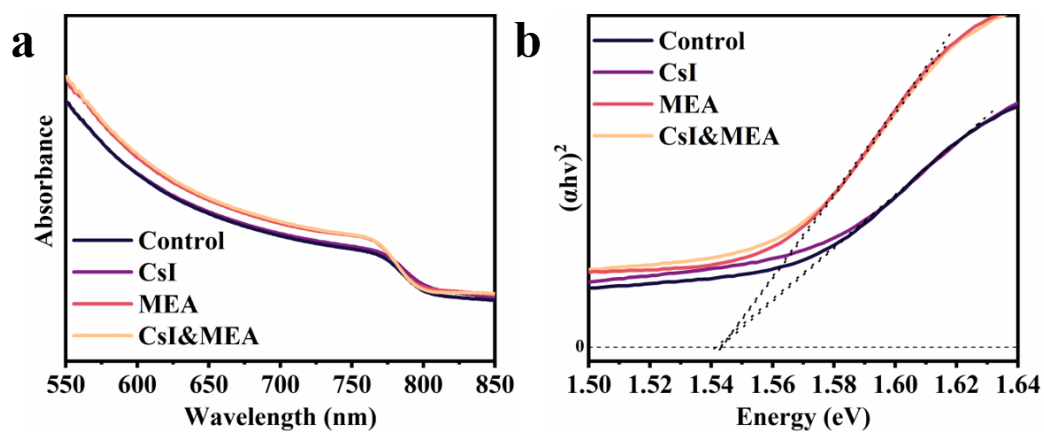


Fig. S17 (a) UV-vis absorption spectroscopy and (b) the optical bandgaps of differently processed perovskite films.

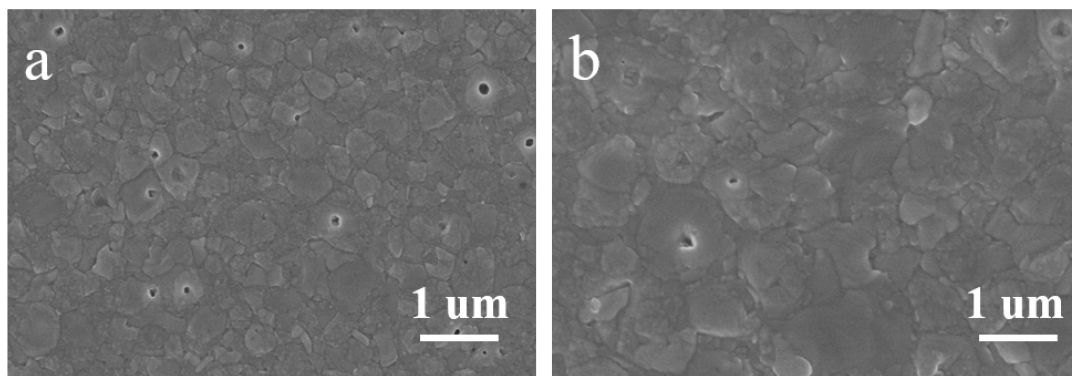
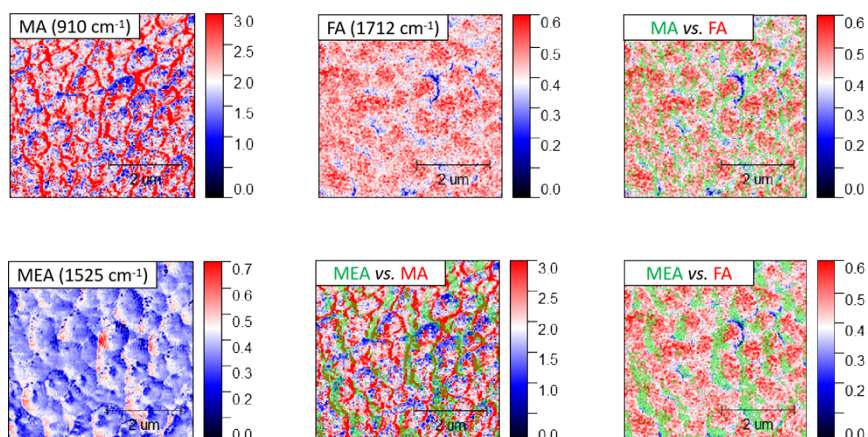


Fig. S18 Top view SEM images of the Control (a) and CsI&MEA (b) perovskite films.

PbI₂ + MEA precursor



PbI₂ + CsI+ MEA precursor

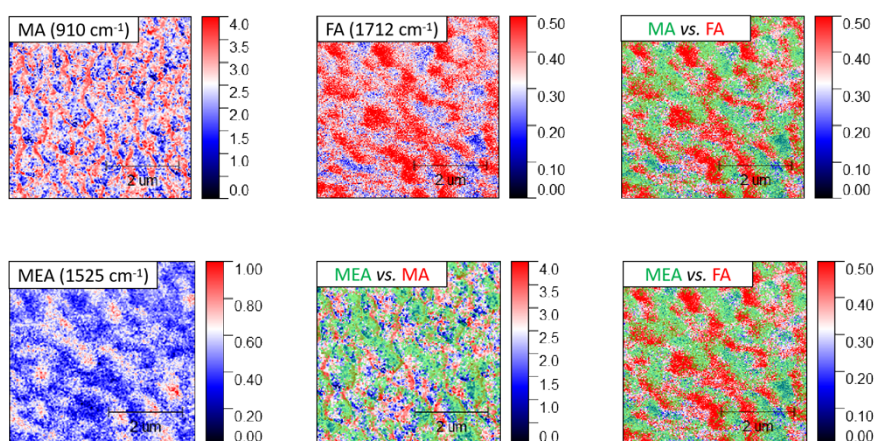


Fig. S19 IR s-SNOM images (red and blue color code) (5 μm × 5 μm) showing the spatial distribution of organic cations (MA, FA) and MEA additive. To visualize the relative distribution of two different components (e.g., MA and FA), one map (green-blue code) is superimposed with another (red-blue code).

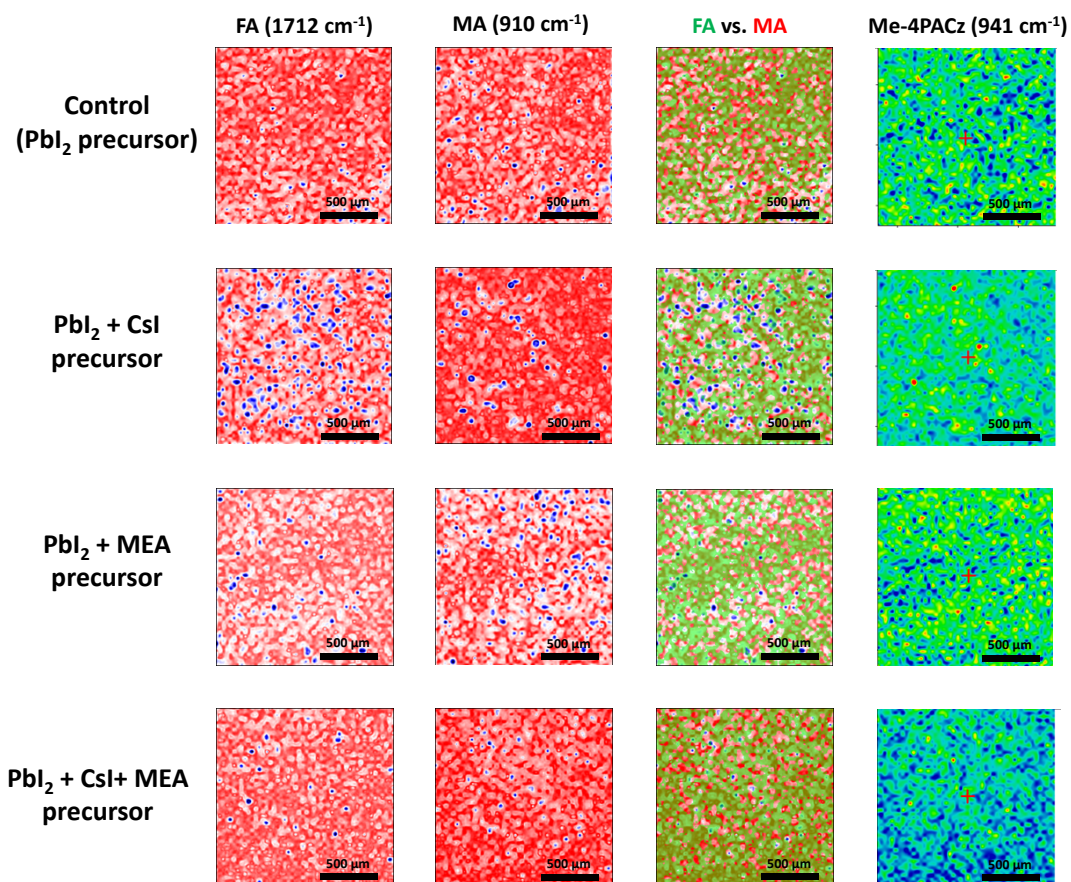


Fig. S20 FTIR mapping results for differently processed perovskite films at the characteristic frequencies of MA (first column), FA (second column) and Me-4PACz (fourth column). The distributions of MA (red) and FA (green) cations are superimposed at the images in the third column.

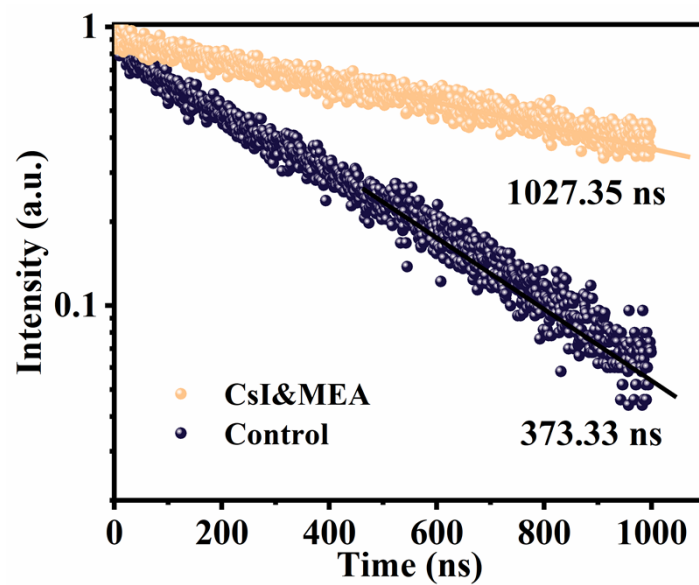


Fig. S21 TRPL spectra of the Control and CsI&MEA perovskite films analyzed using a monoexponential decay fit at the “late part” of the PL decay.

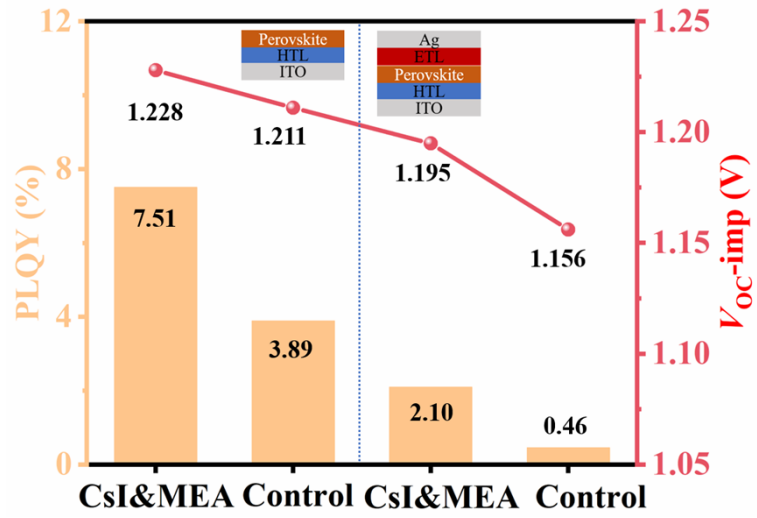


Fig. S22 PLQY results and the obtained V_{oc-imp} of the perovskite films with half-stacks (ITO/HTL/perovskite) and full device stacks for the Control and CsI&MEA perovskite films.

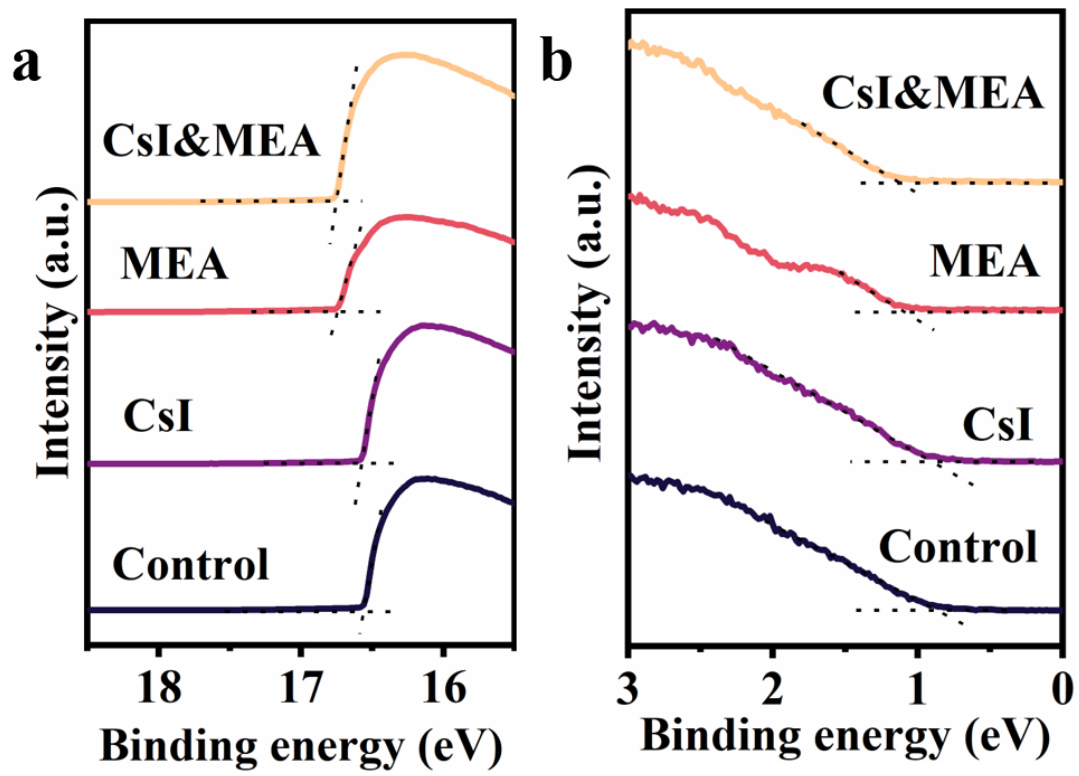


Fig. S23 UPS spectroscopy data: (a) the secondary-electron cut-off binding energy and (b) the valence band region of differently processed perovskite films

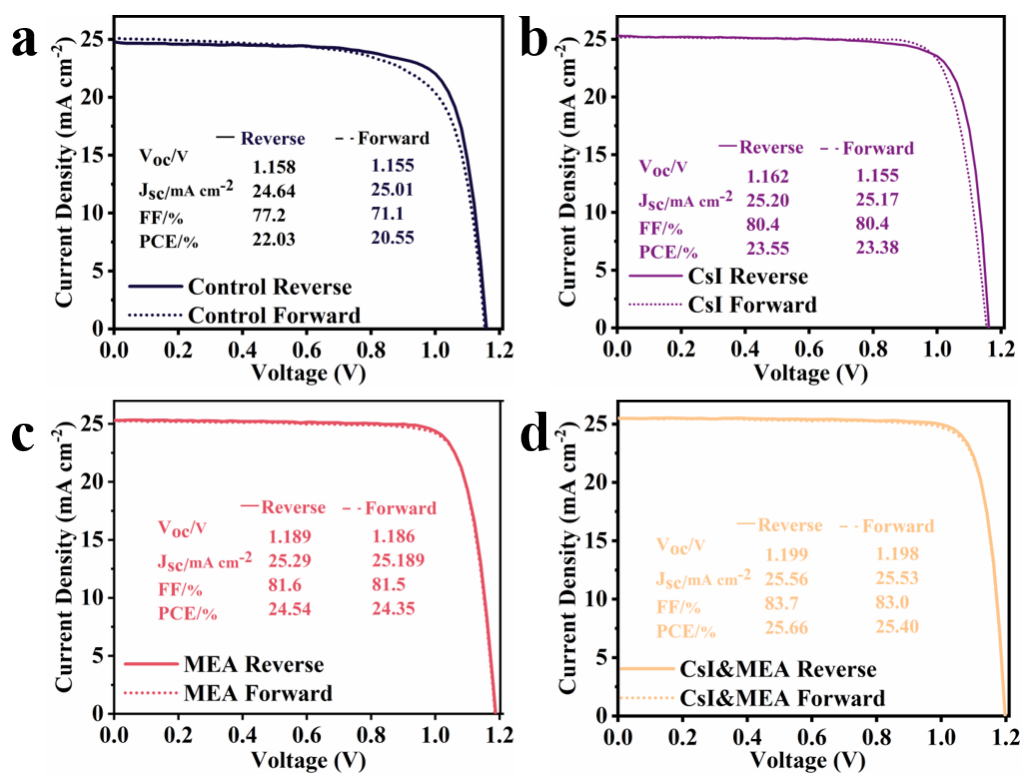


Fig. S24 (a–d) The J - V curves of differently processed perovskite solar cell devices in forward and reverse scan directions.

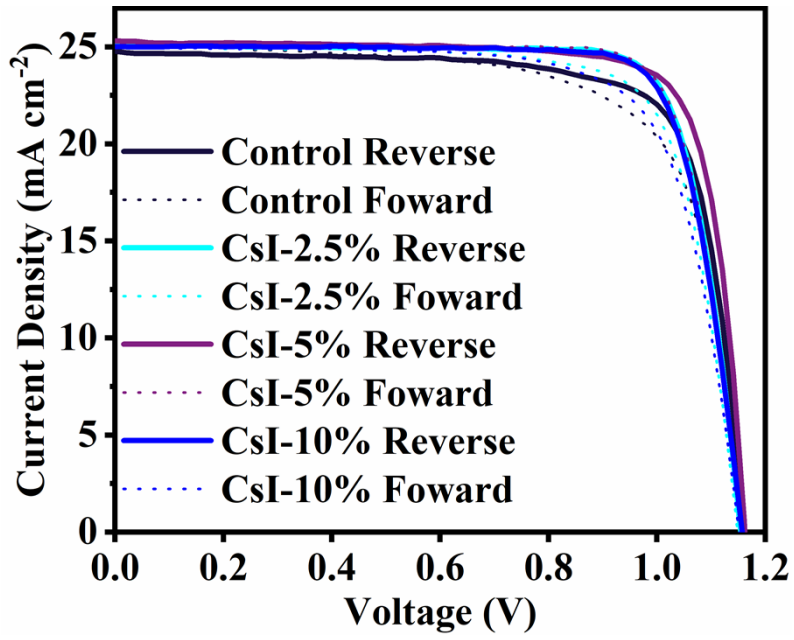


Fig. S25 The J - V curves of the champion PSCs devices assembled using different concentrations of CsI.

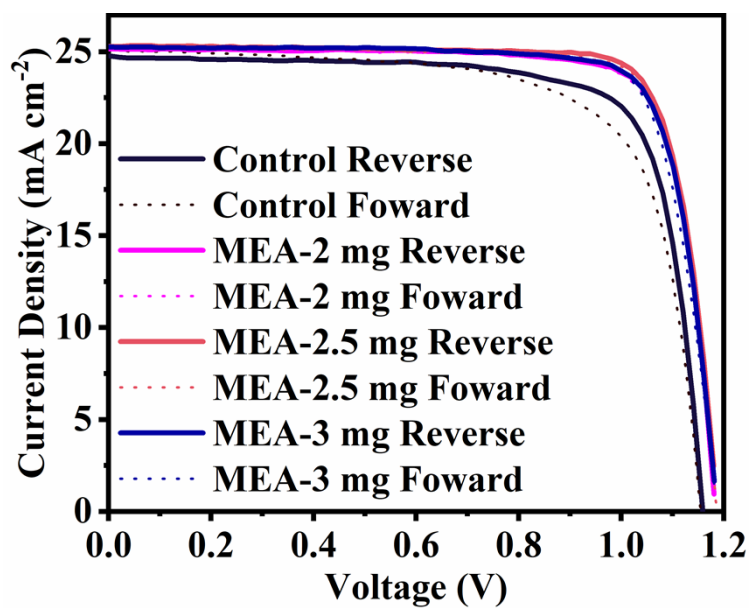


Fig. S26 The J - V curves of the champion PSCs devices assembled using different concentrations of MEA.



No: NBMTEC-SC-241226-0054

No: NBMTEC-SC-241226-0054

New Materials Testing and Evaluation Platform
Zhejiang Regional Center
Ningbo New Materials Testing and Evaluation Center

TEST REPORT

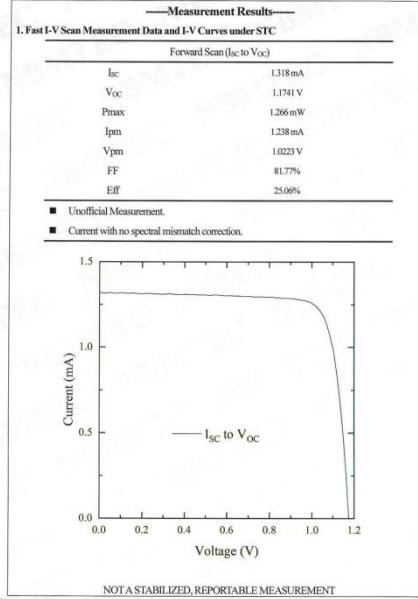
Entrusting Party: Guangzhou Institute of Energy Conversion, CAS
Address of Entrusting Party: No. 2 Nengyuan Road, Tianhe District, Guangzhou City, Guangdong Province, China
Sample Name: Perovskite solar cell
Test Date: 23rd December, 2024



COMPILED BY: [Signature]
REVIEWED BY: [Signature]
APPROVED BY: [Signature]
APPROVED DATE: 2024. 12. 26

Address: Room 1-2, No.21, Building 3, East District, New material innovation center, Ningbo National Hi-Tech Zone,
Ningbo, Tel: 0574-87528296 Post code: 315201

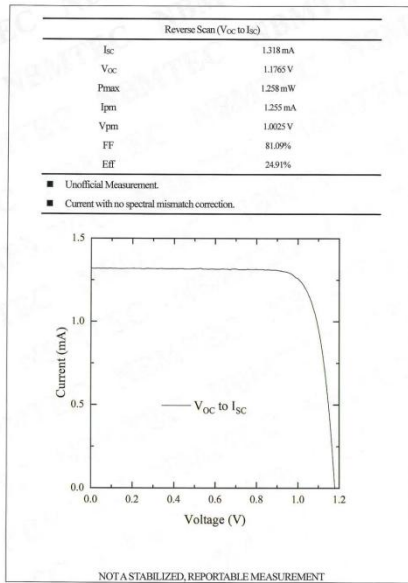
Statement: 1. The test result presented in this report relate only to the object tested.
2. This test report may not be copied or partially interpreted without the written approval of the laboratory.
3. Any dissonance should be demurred within 15 days.



Statement: 1. The test result presented in this report relate only to the object tested.
2. This test report may not be copied or partially interpreted without the written approval of the laboratory.
3. Any dissonance should be demurred within 15 days.

3 / 5

No: NBMTEC-SC-241226-0054



Statement: 1. The test result presented in this report relate only to the object tested.
2. This test report may not be copied or partially interpreted without the written approval of the laboratory.
3. Any dissonance should be demurred within 15 days.

4 / 5

Fig. S27 The certified result for a perovskite solar cell with a PCE of 25.06% provided by Ningbo New Materials Testing and Evaluation Center.

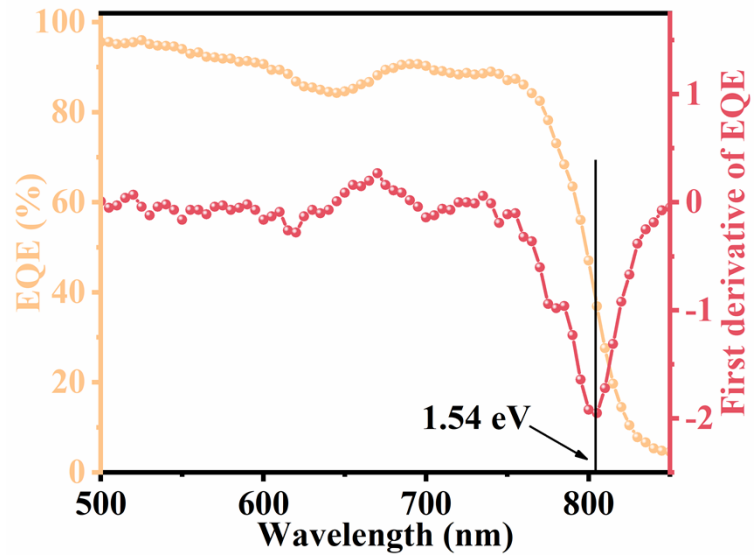


Fig. S28 EQE spectrum and its derivative used for the determination of the bandgap of the CsI&MEA type absorber.

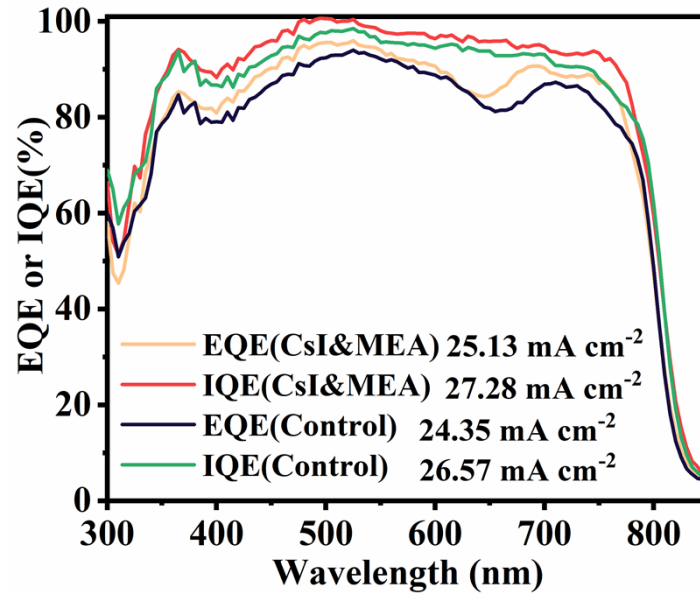


Fig. S29 EQE and IQE spectra with calculated J_{SC} for Control and CsI&MEA devices.

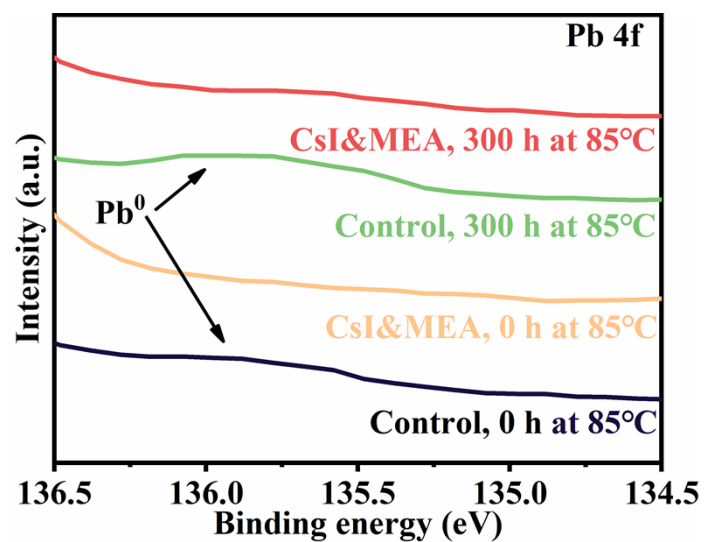


Fig. S30 Pb 4f XPS core level spectra at the binding energy of around 136 eV of the Control and CsI&MEA perovskite films after thermal stability test within 300 hours at 85°C.

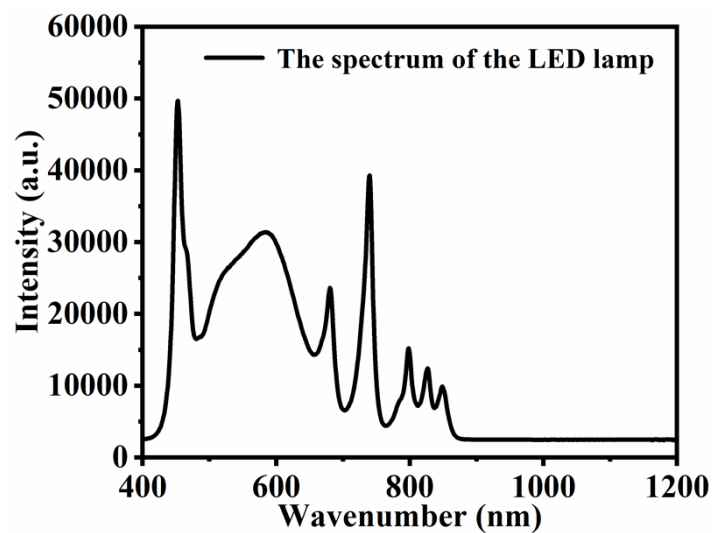


Fig. S31 The spectrum of the LED lamp without ultraviolet part used for the aging test.

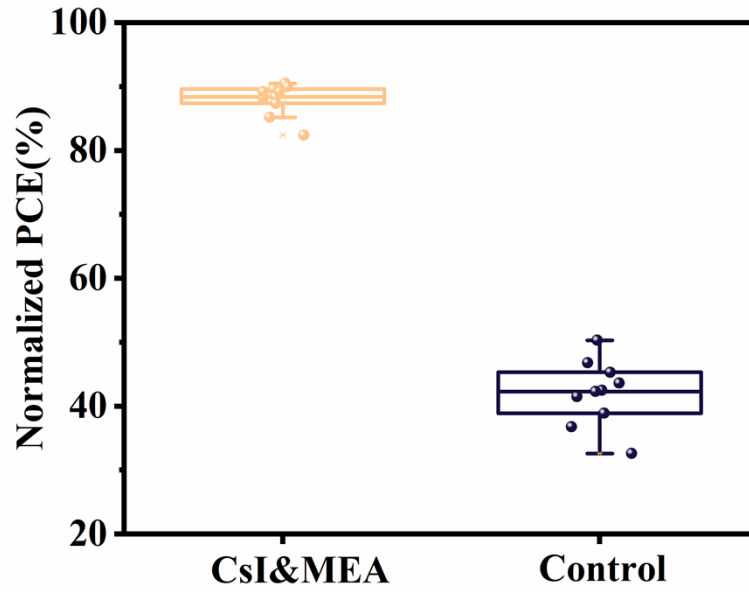


Fig. S32 The normalized PCE distributions for the Control group and the CsI&MEA group samples used for the operational stability tests in MPPT regime under 100 mW cm^{-2} white LED illumination in N_2 . The initial efficiencies of CsI&MEA and control devices are around 25% and 21%, respectively. The statistics were calculated from 10 individual cells.

Table S1 Surface tension of the standard liquids and contact angles for the differently processed PbI₂ films.

Liquid (L)	Surface Tension (mN m ⁻¹)			Contact Angle/ θ (°)			
	Total (γ_L)	Dispersive (γ_L^d)	Polar (γ_L^p)	Control	CsI	MEA	CsI&MEA
Diiodomethane	50.8	50.8	0	35.33	36.10	37.93	38.43
Water	72.3	18.7	53.6	69.44	71.26	73.13	74.45

Table S2 The calculated surface tension of the differently processed PbI₂ films

PbI ₂ film	Surface Tension (mN m ⁻¹)		
	Total (γ_s)	Dispersive (γ_s^d)	Polar (γ_s^p)
Control	49.99	41.87	8.12
CsI	48.90	41.51	7.39
MEA	47.42	40.63	6.79
CsI&MEA	46.68	40.39	6.29

Table S3 Fast and slow components of the PL decay curves and their corresponding ratios for differently processed perovskite films.

Samples	A₁	τ₁(ns)	A₂	τ₂(ns)	τ_{ave} (ns)
Control	0.15	40.84	0.85	455.36	448.66
CsI	0.12	11.64	0.88	795.51	793.98
MEA	0.25	19.36	0.75	1158.68	1152.29
CsI&MEA	0.03	94.28	0.97	1242.98	1240.26

τ_{ave} can be calculated by the equation:

$$\tau_{ave} = \frac{A_1 * \tau_1^2 + A_2 * \tau_2^2}{A_1 * \tau_1 + A_2 * \tau_2}$$

Table S4 Summary on E_{VBM} and E_{CBM} energies of differently prepared perovskite absorber films.

Samples	E_{VBM} (eV)	E_{CBM} (eV)	E_{F} (eV)
Control	-5.54	-4.0	4.67
CsI	-5.56	-4.02	4.66
MEA	-5.59	-4.05	4.49
CsI&MEA	-5.60	-4.06	4.47

Table S5 Performance summary for the champion devices assembled using different concentrations of CsI.

Samples	Scanning direction	V_{OC} (V)	FF (%)	J_{sc} (mA cm ⁻²)	PCE (%)
Control	Reverse	1.158	77.2	24.64	22.03
	Forward	1.155	71.1	25.01	20.55
CsI-2.5%	Reverse	1.153	80.6	25.07	23.29
	Forward	1.152	76.0	25.04	21.92
CsI-5%	Reverse	1.162	80.4	25.20	23.55
	Forward	1.155	80.4	25.17	23.38
CsI-10%	Reverse	1.157	80.0	25.03	23.16
	Forward	1.151	73.9	24.98	21.24

Table S6 Performance summary for the champion devices assembled using different concentrations of MEA.

Samples	Scanning direction	V_{OC} (V)	FF (%)	J_{sc} (mA cm ⁻²)	PCE (%)
Control	Reverse	1.158	77.2	24.64	22.03
	Forward	1.155	71.1	25.01	20.55
MEA-2 mg	Reverse	1.184	80.9	25.14	24.07
	Forward	1.184	80.3	25.11	23.86
MEA-2.5 mg	Reverse	1.189	81.6	25.29	24.54
	Forward	1.186	81.5	25.18	24.35
MEA-3 mg	Reverse	1.186	80.6	25.21	24.11
	Forward	1.186	80.3	25.15	23.95

Table S7 Summary on the photovoltaic parameters of inverted PSCs via sequential deposition method extracted from recent literature on all PSCs.

Year	$E_g(\text{eV})$	$V_{oc}(\text{V})$	FF(%)	$J_{sc}(\text{mA cm}^{-2})$	PCE(%)	Ref.
2022	1.63	1.20	80.4	21.82	21.02	8
2023	1.55	1.13	82.0	25.2	23.4	9
2023	1.56	1.162	82.28	24.47	23.40	10
	1.54	1.199	83.7	25.56	25.66	This work

Table S8 The detailed k and residual tensile stress of different perovskite films.

Samples	k	tensile stress (Mpa)
Control	-0.249	168.2
CsI&MEA	-0.045	30.4

Theoretical References:

- [1] Frisch, M. J.; Trucks, G. W.; Schlegel, H. B.; Scuseria, G. E.; Robb, M. a.; Cheeseman, J. R.; Scalmani, G.; Barone, V.; Petersson, G. a.; Nakatsuji, H.; Li, X.; Caricato, M.; Marenich, a. V.; Bloino, J.; Janesko, B. G.; Gomperts, R.; Mennucci, B.; Hratchian, H. P.; Ortiz, J. V.; Izmaylov, a. F.; Sonnenberg, J. L.; Williams; Ding, F.; Lipparini, F.; Egidi, F.; Goings, J.; Peng, B.; Petrone, A.; Henderson, T.; Ranasinghe, D.; Zakrzewski, V. G.; Gao, J.; Rega, N.; Zheng, G.; Liang, W.; Hada, M.; Ehara, M.; Toyota, K.; Fukuda, R.; Hasegawa, J.; Ishida, M.; Nakajima, T.; Honda, Y.; Kitao, O.; Nakai, H.; Vreven, T.; Throssell, K.; Montgomery Jr., J. a.; Peralta, J. E.; Ogliaro, F.; Bearpark, M. J.; Heyd, J. J.; Brothers, E. N.; Kudin, K. N.; Staroverov, V. N.; Keith, T. a.; Kobayashi, R.; Normand, J.; Raghavachari, K.; Rendell, a. P.; Burant, J. C.; Iyengar, S. S.; Tomasi, J.; Cossi, M.; Millam, J. M.; Klene, M.; Adamo, C.; Cammi, R.; Ochterski, J. W.; Martin, R. L.; Morokuma, K.; Farkas, O.; Foresman, J. B.; Fox, D. J. Gaussian 16 Revision C.01, 2016, Gaussian 16, Revision C.01, Gaussian, Inc., Wallin.
- [2] G. Kresse, J. Hafner, *Physical Review B* 1994, 49 (20), 14251–14269.
- [3] J. P. Perdew, K. Burke, M. Ernzerhof, *Physical Review Letters* 1996, 77 (18), 3865–3868.
- [4] S. Grimme, J. Antony, S. Ehrlich, H. Krieg, *Journal of Chemical Physics* 2010, 132 (15), 154104.
- [5] P. E. Blöchl, *Physical Review B* 1994, 50 (24), 17953–17979.
- [6] G. Kresse, D. Joubert, *Physical Review B* 1999, 59 (3), 1758–1775.
- [7] I. Płowaś-Korus, J. Kaczkowski, *New Journal of Chemistry* 2022, 46 (32), 15381–15391.
- [8] B. Chen, P. Wang, R. Li, N. Ren, W. Han, Z. Zhu, J. Wang, S. Wang, B. Shi, J. Liu, P. Liu, Q. Huang, S. Xu, Y. Zhao, X. Zhang, *ACS Energy Letters*. 2022, 7 (8), 2771-80.
- [9] P. Chen, Y. Xiao, L. Li, L. Zhao, M. Yu, S. Li, J. Hu, B. Liu, Y. Yang, D. Luo, C.H. Hou, X. Guo, J.J. Shyue, Z.H. Lu, Q. Gong, H.J. Snaith, R. Zhu, *Adv Mater*. 2022, 35 (5).

[10]Q. Sun, S. Duan, G. Liu, X. Meng, D. Hu, J. Deng, B. Shen, B. Kang, S.R.P. Silva, *Advanced Energy Materials*. 2023, 13 (36).